MODELLING HEAT AND MASS TRANSFER IN POROUS MATERIAL DURING PYROLYSIS USING OPERATOR SPLITTING AND DIMENSIONLESS ANALYSIS

Julien Maes,[1,*] Ann H. Muggeridge,[1] Matthew D. Jackson,[1] Michel Quintard,[2,3] Alexandre Lapene[4]

[1]Department of Earth Science and Engineering, Imperial College London, U.K.
[2]Université de Toulouse ; INPT, UPS ; IMFT (Institut de Mécanique des Fluides de Toulouse) ; Allée Camille Soula, F-31400 Toulouse, France
[3]CNRS ; IMFT ; F-31400 Toulouse, France
[4]Total CSTJF, Avenue Larribau, 64000 Pau, France

ABSTRACT

Dimensionless analysis is used to improve the computational performance when using operator splitting methods to model the heat and mass transfer during pyrolysis. The specific examples investigated are thermal decomposition of polymer composite when used as heat shields during space-craft re-entry or for rocket nozzle's protection, and the In-Situ Upgrading (ISU) of solid oil shale by subsurface pyrolysis to form liquid oil and gas. ISU is a very challenging process to model numerically because a large number of components need to be modelled using a system of equations that are both highly non-linear and strongly coupled. Inspectional Analysis is used to determine the minimum number of dimensionless groups that can be used to describe the process. This set of dimensionless numbers is then reduced to those that are key to describing the system behaviour. This is achieved by performing a sensitivity study using Experimental Design to rank the numbers in terms of their impact on system behaviour. The numbers are then sub-divided into those of primary importance, secondary importance and those which are insignificant based on the t-value of their effect, which is compared to the Bonferroni corrected t-limit and Lenth's margin of error. Finally we use the sub-set of the most significant numbers to improve the stability and performance when numerically modelling this process. A range of operator splitting techniques is evaluated including the Sequential Split Operator (SSO), the Iterative Split Operator (ISO) and the Alternating Split Operator (ASO).

KEY WORDS: Porous media, Computational methods, Pyrolysis, Dimensionless analysis, Operator splitting

1. INTRODUCTION

Modelling the thermal decomposition in porous media by pyrolysis is challenging because the outcome of this process depends upon a large number of physical mechanisms and their parameters. Many of these parameters are uncertain, e.g. the reaction constants and the temperature dependence of the material properties [9, 10]. In addition, the relative importance of these parameters depends upon the application. Examples of such applications include thermal decomposition of polymer composites when used as heat shields during spacecraft re-entry or for rocket nozzle's protection [2, 11], wood and biomass pyrolysis for heat generation [16], or In-Situ Upgrading of oil shale or heavy oil [5, 18].

Numerical simulation is typically used to predict the outcome of these processes, calibrated and validated by

*Corresponding Julien Maes: j.maes12@imperial.ac.uk

reference to laboratory studies. In most cases these laboratory investigations are performed on different length scales and under different conditions from the planned application and so their results cannot be used directly in designing that application [11]. Before the advent of numerical simulation, dimensionless numbers were often used to scale laboratory results to the application length scale and conditions. These were developed using techniques such as Dimensional Analysis (DA) [26] and Inspectional Analysis (IA) [27].

Despite the advent of faster and more powerful computers, numerical simulation of the outcome of the pyrolysis of porous media remains challenging because of the large number of processes that need to be modelled and the non-linearity of the equations describing these processes. Accurate prediction is further complicated by the fact that many of the inputs needed to describe these processes are uncertain, e.g. the reaction constants and the temperature dependence of the material properties [9, 11]. As well as scaling from laboratory to application scale, dimensionless numbers can also be used to identify the key processes in a given application, thus enabling the development of more efficient numerical schemes.

Various methods for reducing the Central Processing Unit (CPU) time in simulations involving thermal compositional flow coupled with chemistry can be considered. One can identify several numerical operators in the simulation of such processes: heat transport and diffusion, mass transport, and chemical reactions. The time constant of the system is driven by the most penalizing operator. Decoupling techniques, or so-called operator splitting methods, provide a framework to deal separately with each operator and then propose a dedicated resolution (special numerical schemes, explicit/implicit) that leads to smaller systems and more efficient resolution.

Operator splitting is a widely used method for solving reactive transport problems [6, 14]. The basic idea is to split the original problem into a sequence of smaller problems. However, a significant drawback of splitting technique is that decoupling the governing equations introduces an additional source of numerical error, known as splitting error [29].

In this paper, Inspectional Analysis was used to determine the minimum number of dimensionless groups that can be used to describe the process. We then described several operator splitting methods to solve the non-linear systems. The set of dimensionless numbers was then reduced to those that are key to describing the non-linear behaviour of the system by performing a sensitivity study using Experimental Design.

2. MATHEMATICAL MODEL AND DIMENSIONLESS NUMBERS

In this work, we developed a model for the thermal decomposition of polymer composite when used for heat shielding during spacecraft re-entry or for rocket nozzle's protection. Figure 1 illustrates our conceptual model of this process as represented in Henderson and Wiecek experiment [11]. Radiative heat flux caused the thermal decomposition and were represented by the incident heat flux on the left end of the domain. The material could exchange heat at both ends by radiation. The boundary pressure on both ends were equal to the initial pressure P_0.

The following assumptions were made:

1. The solid phase decomposes into a non-reactive gas
2. The decomposition gas behaves ideally
3. Gas flows are described by Darcy's law
4. The gas viscosity has a linear dependence on temperature
5. The permeability has a linear dependence on the solid saturation
6. Local thermal equilibrium (LTE) exists between the solid and the decomposition gas

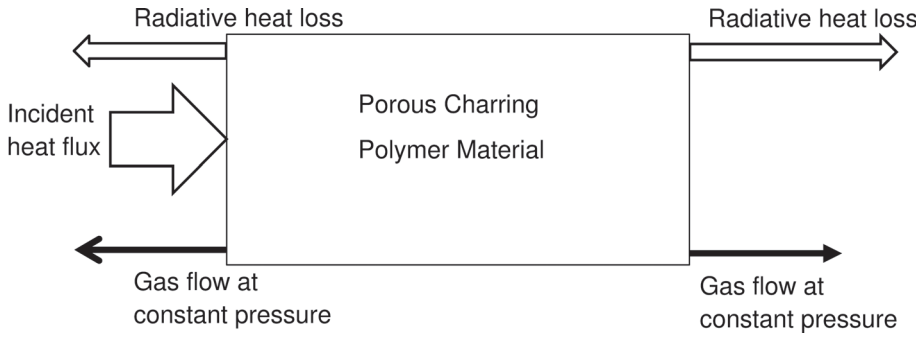

Fig. 1 Model for thermal decomposition of polymer composite as represented in Henderson and Wiecek experiment [11]. Figure from [22].

7. Thermal expansion of the solid is negligible
8. Solid and gas heat capacities and thermal conductivities are constant
9. The thermal conductivities of the inert solid and the solid phase are equal.

These assumptions have been discussed in previous work [7, 11, 16, 22, 25]. They allow the system to be described by only the pressure P, the temperature T, the solid saturation S_s and the gas saturation S_g. The rate of decomposition was modelled using an Arrhenius law of order n:

$$\frac{\partial \phi \rho_s S_s}{\partial t} = -A \left(\phi \rho_s S_s\right)^n \exp\left(-\frac{E_a}{RT}\right) \tag{1}$$

The total mass conservation equation was:

$$\frac{\partial \phi \rho_g S_g}{\partial t} = -\frac{\partial \rho_g v_g}{\partial x} - \frac{\partial \phi \rho_s S_s}{\partial t} \tag{2}$$

The left-hand side of equation (2) is the rate of mass accumulation of gas in the pores. The first term on the right represents the rate of change of the mass flow and the last term the rate of gas generation by pyrolysis. The ideal gas equation of state was used for gas density:

$$\rho_g = \frac{M_g P}{RT} \tag{3}$$

The velocity of the gas was given by Darcy's law:

$$v_g = -k_s \frac{K}{\mu_g} \frac{\partial P}{\partial x} \tag{4}$$

with the gas viscosity given by:

$$\mu_g = \mu_{g,0} + \frac{\partial \mu_g}{\partial T} \left(T - T_0\right) \tag{5}$$

and the solid mobility multiplier k_s:

$$k_s = 1 - \frac{K - K_0}{K} \frac{S_s}{S_{s,0}} \tag{6}$$

Assuming LTE, the energy conservation equation was:

$$\frac{\partial}{\partial t} \left(\left(1 - \phi\right) \rho_I \gamma_I + \phi \rho_s S_s h_s + \phi \rho_g S_g h_g\right) = -\frac{\partial}{\partial x} \left(\rho_g v_g h_g\right) - \frac{\partial q}{\partial x} - \Delta h_r \frac{\partial \phi \rho_s S_s}{\partial t} \tag{7}$$

The first term in Equation (7) is the rate of energy accumulation in the domain; the second term represents the rate of energy transferred by convection; the third term represents the rate of energy transferred by conduction; the last term accounts for energy consumption or generation by chemical reaction. This equation was modified by expanding the accumulation and convection terms and then substituting in the mass conservation equation (2), to yield:

$$\left(\left(1-\phi\right)\rho_I\gamma_I+\phi\rho_s S_s\gamma_s+\phi S_g\rho_g\gamma_g\right)\frac{\partial T}{\partial t}=-\rho_g v_g\gamma_g\frac{\partial T}{\partial x}-\frac{\partial q}{\partial x}-\left(\Delta h_{r0}+h_s-h_g\right)\frac{\partial\phi\rho_s S_s}{\partial t} \tag{8}$$

Finally, the heat flow by conduction q was modelled by Fourier's law:

$$q=-\left(\left(1-\phi\right)\kappa_s+\phi\kappa_s S_s+\phi\kappa_g S_g\right)\frac{\partial T}{\partial x} \tag{9}$$

In Equation 9, we adopted for convenience a simple estimate of the effective thermal conductivity which depends on the volume fraction of the solid and gas in the material. This approximation was previously used in Bennon and Incropera [4]. More complex expressions would not fundamentally change the analysis. Equations (1), (2), (4), (8) and (9) formed a set of coupled non-linear equations to be solved simultaneously for P, T, S_s, v_g and q.

For the heat flow boundary conditions, we assumed constant flux with heat loss by radiation. This gave:

$$\begin{aligned}&\text{at}\quad x=0\quad\forall t\\&q=q_i-\epsilon_s\sigma T^4\\&\text{at}\quad x=L\quad\forall t\\&q=-\epsilon_s\sigma T^4\end{aligned} \tag{10}$$

For the mass flow boundary conditions, we assumed constant pressure equal P_0. This gave:

$$\begin{aligned}&\text{at}\quad x=0\quad\forall t\\&P=P_0\qquad\text{or}\qquad v_g=0\\&\text{at}\quad x=L\quad\forall t\\&P=P_0\qquad\text{or}\qquad v_g=0\end{aligned} \tag{11}$$

Finally, we applied the following initial conditions:

$$\begin{aligned}&S_s=S_{s,0}\\&T=T_0\qquad\text{at}\quad t=0\quad\forall x\\&P=P_0\end{aligned} \tag{12}$$

Next, we used Inspectional Analysis (IA) to determine the set of dimensionless numbers that fully describe our mathematical model. This work is described in more details in Maes et al [22]. By employing their method, we obtained a minimal form of the dimensionless groups [27]. The groups are summarized in Table 1, where τ is defined as the time scale of thermal diffusion in the domain:

$$\tau=\frac{\left(1-\phi\right)\rho_I\gamma_I L^2}{\kappa_s} \tag{13}$$

The dimensionless numbers defined a scaling relationship between different values of the dimensional parameters. The non-linear behaviour of various numerical methods was then tested by performing a sensitivity analysis with these parameters.

Table 1 Summary of Scaling Groups

Name	Notation	Definition	Description
Damköhler number	D_K	$A\tau\left(\phi\rho_s\right)^{n-1}$	$\frac{\text{chemical reaction rate}}{\text{heat diffusion rate}}$
Arrhenius number	N_a	$\frac{E_a}{R\Delta T}$	$\frac{\text{activation energy}}{\text{potential energy}}$
Reduced reaction enthalpy	Δh_r^*	$\frac{\Delta h_r}{\gamma_s \Delta T}$	$\frac{\text{energy liberated}}{\text{energy stored}}$
Reduced initial temperature	T_0^*	$\frac{T_0}{\Delta T}$	
Reduced final porosity	δ	$\frac{\phi}{\phi_0} = \frac{1}{1-S_{s0}}$	
Reduced final permeability	ξ	$\frac{K}{K_0}$	
Lewis number	L_e	$\frac{\phi \mu_{g,0} \kappa_s}{K_0 P_0 (1-\phi)\rho_I \gamma_I}$	$\frac{\text{heat diffusivity}}{\text{pressure diffusivity}}$
Reduced gas density	ρ_g^*	$\frac{M_g P_0}{\rho_s R \Delta T}$	
Solid specific heat decomposition fraction	$\Delta\gamma_s^*$	$\frac{\phi \rho_s \gamma_s}{(1-\phi)\rho_I \gamma_I}$	
Reduced gas specific heat	γ_g^*	$\frac{\gamma_g}{\gamma_s}$	
Reduced gas viscosity derivative	$\Delta\mu_g^*$	$\frac{\partial \mu_g}{\partial T}\frac{\Delta T}{\mu_{g,0}}$	
Gas heat conductivity reduction factor	$\Delta\kappa_g^*$	$\frac{\phi_0(\kappa_s - \kappa_g)}{\kappa_s}$	
Radiative heat loss number	ϵ^*	$\frac{\epsilon_s \sigma \Delta T^3}{\kappa_s}$	$\frac{\text{radiative heat loss}}{\text{heat flux by conduction}}$
Reaction order	n		

3. OPERATOR SPLITTING METHODS

The practice of splitting the reaction and transport steps in simulations of reactive chemical transport has been used in various applications, such as groundwater transport simulations [3], air pollution modelling [19] and combustion-reaction problems [24]. Operator splitting methods provide a framework to deal separately with the transport and the chemical reactions. This has two main advantages. First, dedicated solvers can be applied to each operator. IMPES (Implicit Pressure Explicit Saturation) based transport codes can be coupled with chemical reaction models. For example, accurate ODE (ordinary differential equation) solvers can be employed to cope with the sometimes stiff systems of equations describing the chemical reactions. In addition, different time step strategy can be applied to the different operators, and in the case of ODE, local time steps may be used. The second advantage concerns the number of variables necessary to solve each operator. In some cases, the chemical reaction operator depends on variables that do not affect the transport. This happens for example when a solid immobile phase decomposes through pyrolysis. In addition, complex kinetic models sometimes require a large number of component, while the transport step can be described with a small number of pseudo-components [18].

Operator splitting methods have been widely used for linear or quasi-linear operators [8, 12]. The potential of applying these methods to the thermal decomposition of charring material by pyrolysis can improve precision and performance.

In our investigation, we described our methods on the Cauchy problem of the form:

$$\begin{cases} \dfrac{\partial u}{\partial t} = A\left(u\right)u + K\left(u\right)u, \quad t \in (0, T]\,. \\ u(0) = u_0 \end{cases} \tag{14}$$

In (14), A represents the advection and thermal conduction operator, and K the chemical reaction operator. Operator splitting methods offer two distinct approaches.

In a Sequential Non-Iterative Approach (SNIA), each operator is applied once sequentially. The simplest and most common of these methods is the Sequential Split Operator (SSO) [15], which is a sequence of one transport step followed by one chemical step (SSO-AK, equation 15).

$$\begin{cases} \dfrac{\partial u^*}{\partial t} = A\left(u^*\right) u^*, & t \in \left[t^n, t^{n+1}\right]. \\ u^*(t^n) = u(t^n) & \\ \dfrac{\partial u^{n+1}}{\partial t} = K\left(u^{n+1}\right) u^{n+1}, & t \in \left[t^n, t^{n+1}\right]. \\ u^{n+1}(t^n) = u^*(t^{n+1}) & \end{cases} \tag{15}$$

SSO can be done the opposite way with one chemical step followed by one transport step (SSO-KA, equation 16).

$$\begin{cases} \dfrac{\partial u^*}{\partial t} = K\left(u^*\right) u^*, & t \in \left[t^n, t^{n+1}\right]. \\ u^*(t^n) = u(t^n) & \\ \dfrac{\partial u^{n+1}}{\partial t} = A\left(u^{n+1}\right) u^{n+1}, & t \in \left[t^n, t^{n+1}\right]. \\ u^{n+1}(t^n) = u^*(t^{n+1}) & \end{cases} \tag{16}$$

A significant drawback of the SNIA is that decoupling the governing equations introduces an additional source of numerical error, known as splitting error [29]. The splitting error has been studied extensively for linear operators [12], however this findings may not necessarily apply to non-linear systems. For constant linear operators, the error generated by such methods can be linked to the asymmetry of the operator decoupling. The classical SSO can be modified by using two time steps in an effort to cancel the splitting error, as is done in the Strang-Marchuk Split Operator (SMSO, equations 17 and 18) sometime called the Alternate Split Operator (ASO) [28].

$$\begin{cases} \dfrac{\partial u^*}{\partial t} = A\left(u^*\right) u^*, & t \in \left[t^{2n}, t^{2n+1}\right]. \\ u^*(t^{2n}) = u(t^{2n}) & \\ \dfrac{\partial u^{2n+1}}{\partial t} = K\left(u^{2n+1}\right) u^{2n+1}, & t \in \left[t^{2n}, t^{2n+1}\right]. \\ u^{2n+1}(t^{2n}) = u^*(t^{2n+1}) & \end{cases} \tag{17}$$

and

$$\begin{cases} \dfrac{\partial u^{**}}{\partial t} = K\left(u^{**}\right) u^{**}, & t \in \left[t^{2n+1}, t^{2n+2}\right]. \\ u^{**}(t^{2n+1}) = u^{2n+1}(t^{2n+1}) & \\ \dfrac{\partial u^{2n+2}}{\partial t} = A\left(u^{2n+2}\right) u^{2n+2}, & t \in \left[t^{2n+1}, t^{2n+2}\right]. \\ u^{2n+2}(t^{2n+1}) = u^{**}(t^{2n+2}) & \end{cases} \tag{18}$$

The second category of operator splitting methods is the Sequential Iterative Approach (SIA), which attempts to eliminate or control the splitting error through an iterative process. Unlike SNIA, each sub-step of an iterative scheme solves an approximation to the fully coupled PDE system. The simplest of these methods is the Iterative Split Operator (ISO). In this work, we focused our investigation on SNIA.

Pyrolysis of polymer composites and ISU of oil shale are two processes which are challenging to simulate numerically because they involve the non-linear coupling of chemical reactions and advection. In this paper we investigate the application of operator splitting to these processes, focussing specifically on simulating the experiments of Henderson and Wiecek [11]. They investigated the decomposition of a polymer composite at high temperatures, also developing a 1D numerical model to describe the process, which is similar to the one

presented in this paper but also accounts for the thermal expansion of the material and the evolution of the thermal properties (heat capacity and thermal conduction) with the temperature. The model was validated by performing laboratory experiments using basic phenolic resin, which displays typical decomposition behaviour for glass-filled composites and is used in a large number of high-temperature protection systems [7, 10]. The experimental study was conducted using a 3 cm thick slab. The pressure at both ends, as well as the initial pressure, was 1×10^5 Pa and the initial temperature was 24 ^oC. The solid and gas properties, along with the initial and boundary conditions that we used in our simulation are summarized in Table 2.

Table 2 Summary of parameters for test case 1

Property	Test Case 1
Length L (cm)	3.0
Initial porosity ϕ_0	0.113
Final porosity ϕ_f	0.274
Initial permeability K_0 (m^2)	2.6×10^{-18}
Final permeability K_f (m^2)	2.19×10^{-16}
Inert solid density ρ_I (kg/m^3)	1981.5
Solid phase density ρ_s (kg/m^3)	2304
Inert solid specific heat capacity γ_I (kJ/kg)	2.0
Solid phase specific heat capacity γ_s (kJ/kg)	2.0
Solid thermal conductivity κ_s $(W/m/K)$	1.2
Activation energy E_a $(kJ/kmol)$	2.6×10^5
Pre-exponential factor A $(1/s)$	1.26×10^{-24}, $S_s \geq 0.33$
	44.41, $0.33 \geq S_s \geq 0.0$
Order of reaction n	17.33, $S_s \geq 0.33$
	6.3, $0.33 \geq S_s \geq 0.0$
Heat of decomposition Δh_r (kJ/kg)	234.0
Gas molecular weight M_g $(kg/kmol)$	18.35
Gas initial viscosity $\mu_{g,0}$ $(Pa.s)$	1.54×10^{-5}
Gas viscosity derivative $\frac{\partial \mu_g}{\partial T}$ $(Pa.s/K)$	2.5×10^{-8}
Gas specific heat capacity γ_g (kJ/kg)	3.0
Gas thermal conductivity κ_g $(W/m/K)$	0.1
Initial pressure P_0 (Pa)	10^5
Initial temperature T_0 (^0C)	24
Emissivity ϵ	0.85
Incident heat flux q_i (W/m^2)	2.8×10^5

First, we solved the full system of equations with no splitting using an implicit solution technique with the Newton-Raphson algorithm to handle non-linearities [17]. We chose a small dimensionless time step ($\Delta t_D = 10^{-5}$) in order to obtain a reference solution. Figure 2 compares our simulated predictions of the temperature, pressure and total solid mass (inert and reactant) profiles with those obtained experimentally and numerically by Henderson and Wiecek [11].

Our simulation model did not include thermal expansion, unlike the model of Henderson and Wiecek [11]. To compare the numerical results with ours, we plotted the temperature evolution for different initial position x_0 of the control volumes (figure 2a). The values of the thermal properties of the solid and gas (heat capacity and thermal conductivity) were chosen so that the temperature profiles were similar [22]. This resulted in similar profiles for the dimensionless pressure and the solid mass fraction (figures 2b and 2c).

We then studied the evolution of the relative error between our reference solution (using the fully implicit Newton method) and the three SNIA described above (SSO-AK, SSO-KA and SMSO). We used the following

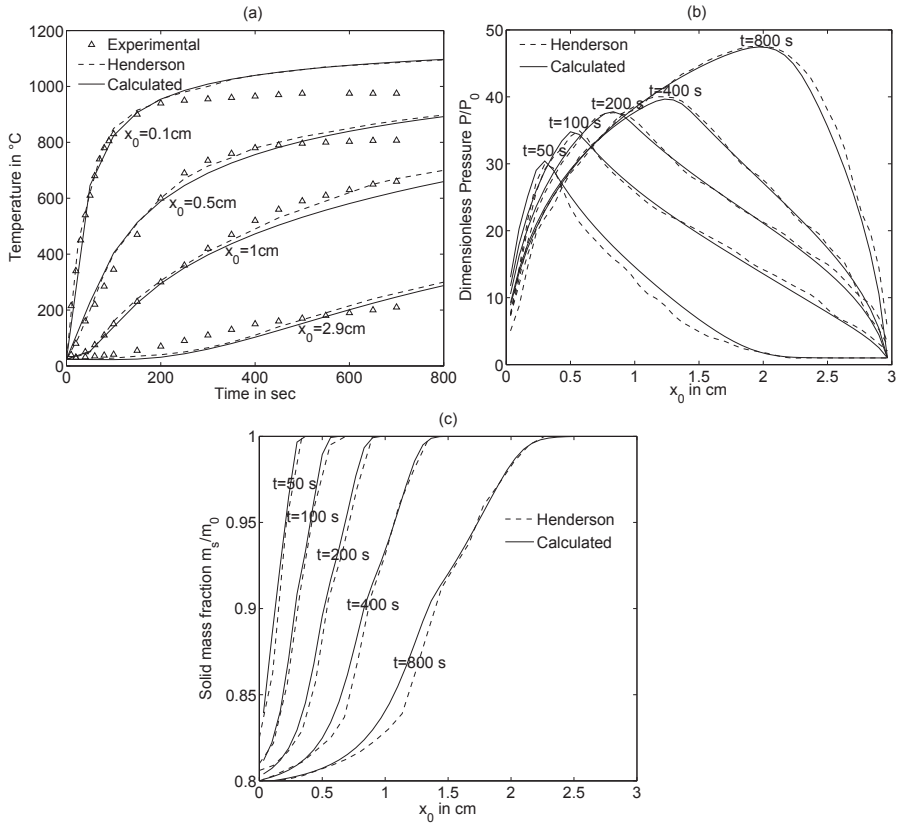

Fig. 2 Figure (a) shows the temperature evolution for various initial positions, figure (b) shows pressure profile in the domain at various times and figure (c) shows the solid mass fraction profile in the domain at various times. We observed good agreement between our numerical results and Henderson's experimental and numerical simulation results

definitions for the normalized error for each variable:

$$err_P = \max_n \left(\frac{1}{n_d} \sum_{x_j} \frac{|P(t^n, x_j) - P_{ref}(t^n, x_j)|}{P_0} \right) \tag{19}$$

$$err_T = \max_n \left(\frac{1}{n_d} \sum_{x_j} \frac{|T(t^n, x_j) - T_{ref}(t^n, x_j)|}{\Delta T} \right) \tag{20}$$

$$err_S = \max_n \left(\frac{1}{n_d} \sum_{x_j} |S_g(t^n, x_j) - S_{g,ref}(t^n, x_j)| \right) \tag{21}$$

For this simple example, we used the Newton-Raphson algorithm for both operators, so the only performance improvement concerned the number of variables. For the fully implicit scheme, we needed to solve for pressure, temperature and gas saturation for each non-linear iterations. The complexity of the algorithm was $\sim n_v \log(n_v)$ where n_v is the number of variables, so we estimated the CPU time for one non-linear iteration using $3n_d \log(n_d)$ with n_d the number of control volumes in our discretization scheme. For the splitting methods, we neglected the CPU cost of the chemical reaction operator because it was fully local. Its resolution complexity was $\sim n_v$ and it could be solved simultaneously on all control volumes. Therefore, the estimated CPU time for the splitting method was the estimated CPU time for the advection-conduction operator. We used

an IMPES scheme with implicit temperature to solve the transport step, so the estimated CPU time for one transport iteration was $2n_d \log(n_d)$

Figure 3 shows the evolution of the normalized errors with the dimensionless time step and the estimated CPU time. We observed that the SSO-AK gave a non-physical pressure error. The pressure rose during a chemical reaction step and can reach non-physical values if not relaxed by a transport step afterwards. However, we obtained a small saturation error. On the other hand, SSO-KA had a limited pressure error but the saturation error was large. SMSO gave an interesting compromise between the two methods but the pressure error was still too big.

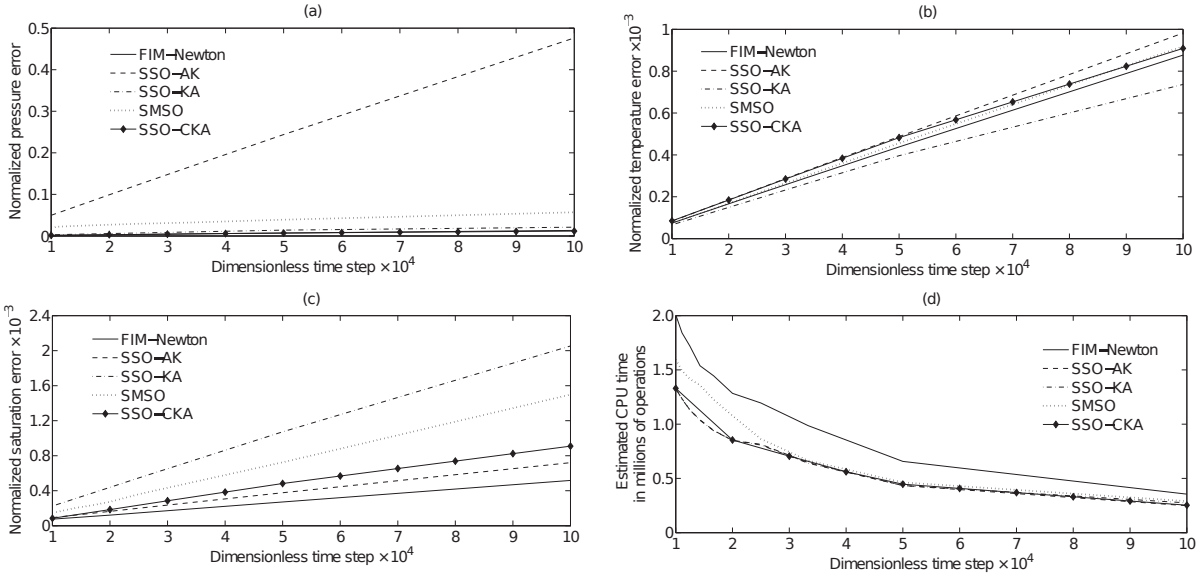

Fig. 3 Figure (a) shows the evolution of the normalized pressure error, figure (b) the evolution of the normalized temperature error and figure (c) the evolution of the normalized saturation error with respect to the time step size. We observed that the SSO-CKA gives the best compromise in term of error for the pressure, the temperature and the saturation. Figure (d) shows the advantage of the splitting methods in term of estimated CPU time

Looking more closely at the error arising from the SSO-KA splitting, we observed that the main component was coming from the temperature in the chemical reaction step. Indeed, the operator K was performed with a temperature that had not been transported yet. As the thermal conduction was the dominant process controlling the temperature, we tried to solve this problem by using a splitting scheme where the thermal conduction was performed first (operator C), followed by a chemical reaction step (operator K) and finally the advection part with no thermal conduction (operator A'). This method was defined as SSO-CKA (equation 22).

$$\begin{cases} \dfrac{\partial u^*}{\partial t} = C\left(u^*\right) u^*, & t \in \left[t^n, t^{n+1}\right]. \\ u^*(t^n) = u(t^n) & \\ \dfrac{\partial u^{**}}{\partial t} = K\left(u^{**}\right) u^{**}, & t \in \left[t^n, t^{n+1}\right]. \\ u^{**}(t^n) = u^*(t^{n+1}) & \\ \dfrac{\partial u^{n+1}}{\partial t} = A'\left(u^{n+1}\right) u^{n+1}, & t \in \left[t^n, t^{n+1}\right]. \\ u^{n+1}(t^n) = u^{**}(t^{n+1}) & \end{cases} \tag{22}$$

The evolution of the normalized errors with the dimensionless time step for SSO-CKA was also plotted on figure 3. We observed that it gave the best compromise in term of error for the pressure, the temperature and the saturation. Figure (d) shows the advantage of the splitting methods in term of estimated CPU time. For SSO-CKA, we needed to solve an additional transport step for the thermal conduction (complexity $\sim n_d \log(n_d)$), but because we removed the thermal conduction from the advection step, the temperature could be treated explicitly in the advection step [21]. Therefore, the estimated CPU for the SSO-CKA was equivalent to the estimated CPU of SSO-KA.

We concluded that the SSO-CKA was showing many advantages when applied to Henderson and Wiecek's experiment. The splitting error was small compared to those arising from the other SNIA. The estimated CPU time was reduced compared to the fully implicit Newton method, and the time discretization error could be reduced by using dedicated solver and local time stepping for the reaction step. However, due to robustness, this method could not be applied to any test case without an algorithm to control the splitting error.

4. EVALUATION OF COMPUTATIONAL EFFICIENCY USING EXPERIMENTAL DESIGN

The objective of using operator splitting for these problems is to improve computational speed whilst maintaining accuracy. This can only be achieved by choosing the largest possible time step that is consistent with minimizing the splitting error. Unfortunately, the splitting error can not be evaluated a priori especially for non-linear system. However, we can study it as a function of the physical parameters using the dimensionless numbers to characterise for which values of those numbers the splitting error is small and SNIA can be used.

The objective of this part of our study is to identify the primary dimensionless groups that influence the splitting error of the SSO-CKA method. For this, we used a general algorithm for adapting the time step size to control the time discretization error. The algorithm used an a posteriori error estimator derived from two solutions, one obtained using a full-size time step Δt, and one using two time steps $\Delta t/2$ [8].

The time discretization error for the approximate solution u_1 obtained with a single time step of size Δt using a fully implicit Newton or SSO-CKA is:

$$u\left(t^{n+1}\right) - u_1\left(t^{n+1}\right) = \lambda\left(\Delta t\right)^2 + O(\Delta t)^3 \tag{23}$$

where $u(t^{n+1})$ is the exact solution, n is the time index and λ is a constant. Similarly, for the approximate solution u_2, we applied two consecutive time steps of size $\Delta t/2$. The time discretization error is:

$$u\left(t^{n+1}\right) - u_2\left(t^{n+1}\right) = 2\lambda\left(\frac{\Delta t}{2}\right)^2 + O(\Delta t)^3 \tag{24}$$

Subtracting the two equations and solving for λ, we obtain:

$$\lambda = \frac{2}{\Delta t^2}\left(u_2^n - u_1^n\right) \tag{25}$$

So the order 2 error estimate for u_2 is:

$$\epsilon = \frac{1}{n_d}\sum_{i=1}^{nd} |u_{2,i}^{n+1} - u_{1,i}^{n+1}| \tag{26}$$

where the sum is applied to the n_d control volumes. This error is then used to control the time step in order to

limit the discretization error using:

$$\Delta t^{n+1} = min\left\{ f_s \Delta t^n \sqrt{\left(\frac{\epsilon_a}{\epsilon}\right)}, f_m \Delta t^n \right\} \tag{27}$$

where ϵ_a is the error tolerance, $f_s \leq 1$ is a safety factor intended to reduce solver failures due to inaccuracies in the error estimation, and $f_m \geq 1$ is a maximum time step growth rate factor

In this case the method is used to investigate the dependency of the splitting error with the physical parameters of the problem. Since the time step size is controlled by the estimated time discretization error (equation 27), the difference between the number of time steps performed by SSO-CKA and the number of time steps performed by the fully implicit Newton method depends on the splitting error. Let:

$$y = \frac{\text{number of time iterations with SSO-CKA - number of time iterations with FIM-Newton}}{\text{number of time iterations with FIM-Newton}} \tag{28}$$

When y is high, it means that SSO-CKA uses smaller time steps than the fully implicit Newton method for similar time discretization error. This is a consequence of a large splitting error. When y is small, it means that the time discretization error for SSO-CKA and fully implicit Newton method are similar when used with similar time steps and so the splitting error is small. We conclude that y is a measure of the splitting error of SSO-CKA.

We decided to use Experimental Design to investigate y as a function of system inputs. We performed a sensitivity analysis with the fourteen dimensionless groups as our system parameters. The procedure for a sensitivity analysis is:

1. Choose the type of Experimental Design
2. Determine a range for each parameter
3. Perform the experimental trials
4. Calculate the main and interaction effects
5. Determine which parameters are important in characterising system performance

In this study, we applied a first-order response surface model with interactions [23]:

$$y = \beta_0 + \sum \beta_i x_i + \sum_{i \neq j} \beta_{ij} x_i x_j \tag{29}$$

where y is the response analysed and x_i the factors of interest. The β_i terms are called main factor effects and the β_{ij} terms the two-factor interaction effects. In this study, we used a two-level fractional factorial design of resolution V. Algorithms to generate a design of resolution V were described in Myers et al. [23]. The results of the sensitivity analysis depend only on the resolution of the design and not on the choice of the generators.

We selected a design of resolution V comprising $n = 2^8$ trials. The next task was to evaluate a range for each scaling group. Table 3 defines a minimum and maximum value for each dimensional parameter taken from the literature [7, 11]. We then obtained a range for our fourteen dimensionless groups (table 4).

We then performed the experimental trials and computed the main effects β_i and the interaction effects β_{ij} using the least squares method [23]. In order to obtain a normalized measure of the impact, we computed the t-value of each effect, which is simply the numerical effect divided by its associated standard error [13]. Figure 4a shows the t-value of the main effects and Figure 4b shows the t-value of the twelve most important interaction effects.

Table 3 Range of values for the various dimensional parameters of the thermal decomposition of polymer composite model

Property	min	max	Property	min	max
$L\,(cm)$	1	10	ϕ	0.1	0.3
ϕ/ϕ_0	2	4	$K/\phi\,(m^2)$	10^{-15}	10^{-13}
K/K_0	40	800	$\rho_I\,(kg/m^3)$	1500	2000
$\gamma_I\,(kJ/kg)$	1	3	$\kappa_s\,(W/m/K)$	1	2
$\rho_s\,(kg/m^3)$	2000	3000	$\gamma_s\,(kJ/kg)$	1	3
$A\,(\phi\rho_s)^{n-1}\,(1/s)$	10^{16}	10^{22}	E_a(kJ/kmol)	2×10^5	3×10^5
$\Delta h_r\,(kJ/kg)$	100	1000	n	1	50
$\gamma_g\,(kJ/kg)$	2	4	$M_g\,(kg/kmol)$	16	30
$\mu_{g0}\,(Pa.s)$	10^{-5}	2×10^{-5}	$\frac{\partial\mu_g}{\partial T}\,(Pa.s/K)$	10^{-8}	3×10^{-8}
$\kappa_g\,(W/m/K)$	0.05	0.2	ϵ	0.6	0.9
$P_0\,(Pa)$	10^5	10^6	$T_0\,(^0C)$	10	50
$T_i\,(^0C)$	1000	1600			

Table 4 Range of values obtained for the various scaling groups for thermal decomposition of polymer composite. We observe that several numbers, such as L_e, vary over a large range, whereas other numbers, such as T_0^* vary over a much smaller range.

Groups	min	max	Groups	min	max
D_K	7.75×10^{17}	6.90×10^{26}	N_a	15.1	38.0
T_0^*	0.18	0.340	δ	2.00	4.00
ξ	40.0	800	ρ_g^*	4.03×10^{-6}	5.70×10^{-4}
L_e	4.83×10^{-6}	0.26	$\Delta\mu_g^*$	0.47	4.77
$\Delta\gamma_s^*$	0.04	0.72	γ_g^*	0.67	4.0
Δh_r^*	0.02	1.1	$\Delta\kappa_g$	0.08	0.29
ϵ^*	0.15	20.5	n	1	50

In order to classify the importance of the effects, we defined two measures of significance. The first measure compared the t-value of the effect with the critical value $t_{\alpha,d}$ of a student t-distribution with d degrees of freedom and a confidence limit $1-\alpha$ with Bonferroni correction [1, 22]. We obtained the Bonferroni corrected t-value referred as the t-limit:

$$t = t_{0.05/255,150} = 3.8 \tag{30}$$

The second measure referred as the l-limit was defined by the t-value of Lenth's margin of error LME [20] based on a simple formula for the standard error of the effect:

$$l = LME \times t_{0.05,255} = 1.32 \times 1.97 = 2.6 \tag{31}$$

Effects that were smaller than the l-limit were considered to be insignificant (in white in figure 4). Effects that were bigger than the t-limit were considered to be primary (in black in figure 4).

The factors were naturally regrouped into three classes:

- The primary factors: ϵ^*, ρ_g^*, Δh_r^*, $\Delta\gamma_s^*$, and n. These are the factors which have their main effect or at least one of their interaction effects bigger than the t-limit. The splitting error of SSO-CKA applied to the thermal decomposition of polymer composite depends mainly on these five factors and their interactions.
- The secondary factors: D_K, $\Delta\mu_g^*$, $\Delta\kappa_g^*$ and L_e. These are the factors which have no main effect or any interaction effect bigger than the t-limit but their main effect or at least one of their interaction effects is bigger than the l-limit. The effect of the secondary factors is not negligible, but it is reduced compared to the effect of the primary factors.

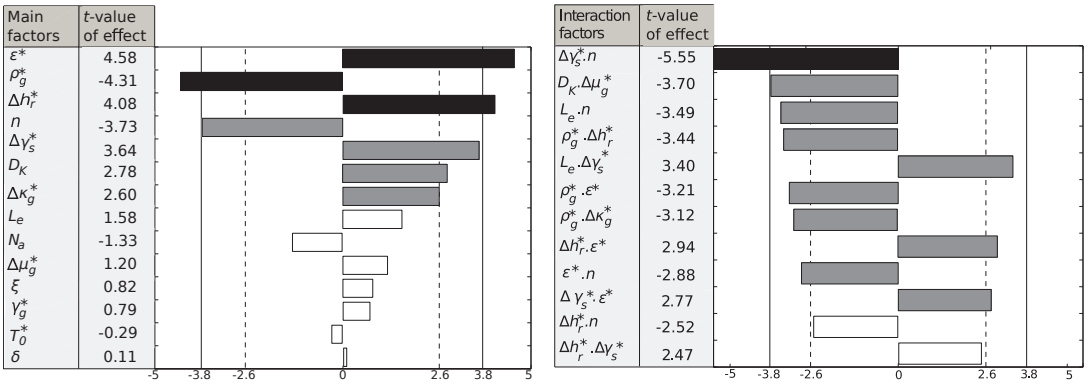

Fig. 4 Variability of time stepping (function y). The various effects were compared with Bonferroni t-limit (in plain line) and Lenth's margin of error l (in dashed line). Primary effects were represented in black, secondary in grey and insignificant in white.

- The insignificant factors: N_a, ξ, γ_g^*, δ and T_0^*. These are the factors which have no main effect or interaction effect bigger than the l-limit.

We concluded that the splitting error arising from SSO-CKA mainly depends on the five primary factors. Hence, the analysis of the performance of SSO-CKA for given system inputes could be restricted to varying those parameters to help identify where SSO-CKA will not be badly affected by splitting error. We observed that SSO-CKA was the most useful for small radiative heat loss number, reduced reaction enthalpy and solid specific heat decomposition fraction, and big reduced gas density and reaction order. With further analysis, one can hope to identify critical values for those parameters for which SSO-CKA or fully implicit Newton method should be used.

5. CONCLUSION

This work focused on the application of several operator splitting methods to solve a thermal reactive transport problem, where solid charring material decomposed into non-reactive gas. We showed that SSO-AK, SSO-KA and SMSO applied to a simple problem from the literature [11] led to important time discretization errors. We proposed to solve this issue with a splitting scheme where the thermal conduction was performed first, followed by a chemical reaction step and finally the advection part with no thermal conduction (SSO-CKA).

SSO-CKA led to small time discretization errors while showing the potential to improve the computation time. However, the method can not be applied to every test cases without controlling the time step. In order to study the effect of the splitting error on the time step, we performed a sensitivity analysis using dimensionless numbers obtained from Inspectional Analysis as our system parameters.

The sensitivity analysis enabled us to divide the dimensionless numbers into three groups (primary, secondary and insignificant) based on the values of the t and l-limits. We concluded that the splitting error for SSO-CKA depended essentially on five primary factors: the radiative heat loss number, the reduced gas density, the reduced reaction enthalpy, the solid specific heat decomposition fraction and the reaction order.

We then could limit the study of the performance of SSO-CKA to those five parameters. Future work could enable us to define more precisely for which part of the parameter space for the modelling of polymer charring the use of SSO-CKA would be recommended. The method could also be applied to the In-Situ Upgrading of oil shale and heavy oil.

Nomenclature

Roman Symbols

A	pre-exponentiel factor ($kmol^{1-n}/s$)
E_a	activation energy (J/mol)
h	specific enthalpy (J/kg)
K	rock permeability (m^2)
k	mobility multiplier (no unit)
L	domain length (m)
M	molecular weight ($kg/kmol$)
P	pressure (Pa)
q	energy flow by conduction (W/m^2)
R	universal gas constant ($8.314\ J/mol/K$)
T	temperature (K)
t	time (s)
v	velocity (m/s)
x	one dimensional coordinate (m)

Greek Symbols

Δh_r	reaction enthalpy (J/kg)
ΔT	temperature scale $\Delta T = T_i - T_0$ (K)
ϵ	emissivity
γ	specific heat capacity ($J/kg/K$)
κ	thermal conductivity ($W/m/K$)
μ	viscosity ($Pa.s$)
ϕ	rock porosity (no unit)
ρ	mass density (kg/m^3)
σ	Stefan-Boltzmann constant ($5.67 \times 10^{-8}\ W/m^2/K^4$)
τ	time scale of heat conduction in porous media (s)

Subscripts

0	initial value
g	gas
I	inert solid
i	incident heat value
s	solid phase

ACKNOWLEDGMENTS

This work was done at Imperial College and is supported by Total S.A.

REFERENCES

[1] Anderson, M. J. and Whitcomb, P. J., *DOE Simplified: Practical Tools for Effective Experimentation*, 2nd Edition, Productivity Press, (2007).

[2] Bai, Y., Vallee, T., and Keller, T., "Modeling of Thermal Responses for FRP Composites Under Elevated and High Temperatures," *Composites Science and Technology*, 68(1), pp. 47–56, (2008).

[3] Barry, D. A., Miller, C. T., Culligan, P., and Bajracharya, K., "Analysis of Split-Operator Methods for Non-Linear and Multispecies Groundwater Chemical Transport Models," *Mathematics and Computers in Simulation*, 43, pp. 331–341, (1997).

[4] Bennon, W. D. and Incropera, F. P., "A Continuum Model for Momentum, Heat and Species Transport in Binary Solid-Liquid Phase Cahnge Systems-I. Model Formulation," *International Journal of Heat and Mass Transfer*, 30(10), pp. 2161–2170, (1987).

[5] Fan, Y., Durlofsky, L., and Tchelepi, H., "Numerical Simulation of the In-Situ Upgrading of Oil Shale," *SPE Reservoir Simulation Symposium, 2-4 February 2009, The Woodlands, Texas, USA*, (2010).

[6] Farago, I., "A Modified Iterated Operator Splitting Method," *Applied Mathematical Modelling 32*, 32, pp. 1542–1551, (2007).

[7] Florio, J., Henderson, J. B., Test, F. L., and Hariharan, R., "A Study of the Effects of the Assumption of Local-Equilibrium on the Overall Thermally-Induced Response of Decomposing, Glass-Filled Polymer Composite," *International Journal of Heat and Mass Transfer*, 34(4), pp. 135–147, (1991).

[8] Gasda, S. E., , Farthing, M. W., Kees, K. E., and Miller, C. T., "Adaptive Split-Operator Methods For Modeling Transport Phenomena in Porous Medium Systems," *Advances in Water Resources*, 34, pp. 1268–1282, (2011).

[9] Gersten, J., Fainberg, V., Hetsroni, G., and Shindler, Y., "Kinetic study of the thermal decomposition of polypropylene, oil shale, and their mixture," *Fuel*, 79(13), pp. 1679–1686, Oct 1999.

[10] Henderson, J. B., Emmerich, W. D., Hagemann, L., and Post, E., "Thermophysical property measurement on a complex high-temperature polymer composite," *High temperatures high pressures*, 25(6), pp. 693–698, (1993).

[11] Henderson, J. B. and Wiecek, T. E., "A Numerical Study of the Thermally-Induced Response of Decomposing, Expanding Polymer Composites," *Wärme und Stoffübertragung*, 22(5), pp. 275–284, (1988).

[12] Herzer, J. and Kinzelbach, W., "Coupling of Transport and Chemical Processes in Numerical Transport Models," *Geoderma*, 44, pp. 115–127, (1989).

[13] Hogg, R. T., McKean, J. W., and Craig, A. T., *Introduction to Mathematical Statistics*, 6th Edition, Pearson Education, Inc, (2005).

[14] Hundsforfer, W. and Verwer, J. G., *Numerical Solution of Time-Dependent Advection-Diffusion-Reaction Equations*, Springer-Verlag, Berlin, Germany, (2003).

[15] Kanney, J. F., Miller, C. T., and Kelley, C. T., "Convergence of Iterative Split-Operator Approaches for Approximating non-linear Reactive Transport Problems," *Advances in Water Resources*, 26, pp. 247–261, (2003).

[16] Kansa, E. J., Perler, H. E., and Chaiken, R. F., "Mathematical Model of Wood Pyrolysis Including Internal Convection Force," *Combustion and Flame*, 29, pp. 311–324, (1977).

[17] Kelley, C. T., *Solving Nonlinear Equations with Newton's Method*, SIAM, (2003).

[18] Kumar, J., Fusetti, L., and Corre, B., "Modeling In-Situ Upgrading of Extraheavy Oils/Tar Sands by Subsurface Pyrolysis," *Canadian Unconventional Resources Conference, 15-17 November 2011, Alberta, Canada*, (2011).

[19] Lanser, D. and Verwer, J., "Analysis of Operator Splitting for Advection-Diffusion-Reaction Problems from Air Pollution Modelling," *Journal of Computational and Applied Mathematics 111 (1999) 201-216*, 111, pp. 201–216, (1999).

[20] Lenth, R., "Quick and Easy Analysis of Unreplicated Factorials," *Technometrics*, 31, pp. 469–473, (1989).

[21] Maes, J., Moncorgé, A., and Tchelepi, H., "Thermal Adaptive Implicit Method: Time Step Selection," *Journal of Petroleum Science and Engineering*, 106(10), pp. 34–45, (2013).

[22] Maes, J., Muggeridge, A. H., Jackson, M. D., Quintard, M., and Lapene, A., "Scaling Heat and Mass transfer in the Presence of Pyrolysis," (2014), currently under review.

[23] Myers, R. H., Montgomery, D. C., and Anderson-Cook, C. M., *Response Surface Methodology: Process and Product Optimization Using Design of Experiments*, 3rd Edition, John Wiley and Sons, Inc., Oxford, (2009).

[24] Pope, S. B. and Ren, Z., "Efficient Implementation of Chemistry in Computational Combustion," *Flow Turbulence and Combustion*, 82(4), pp. 437–453, June 2009.

[25] Puiroux, N., Prat, A., and Quintard, M., "Non-Equilibrium Theories for Macroscale Heat Transfer: Ablative Composite Layer Systems," *International Journal of Thermal Sciences*, 43(6), pp. 541–554, (2004).

[26] Ruzicka, M. C., "On Dimensionless Numbers," *Chemical Engineering Research and Design*, 86(8a), pp. 835–868, (2008).

[27] Shook, M., Li, D., and Lake, W. L., "Scaling Immiscible Flow Through Permeable Media by Inspectional Analysis," *IN SITU*, 16(4), pp. 311–349, (1992).

[28] Strang, G., "On the Constuction and Comparison of Difference Schemes," *SIAM Journal on Numerical Analysis*, 5(3), pp. 506–517, September 1968.

[29] Valocchi, A. J. and Malmstead, M., "Accuracy of Operator Splitting for Advection-Dispersion-Reaction Problems," *Water Resources Research*, 28(5), pp. 1471–1476, Mai 1992.